

Log-Periodic Antenna for Partial Discharge Detection Application

Zulbirri Faizol^{1*}, Farid Zubir^{1*}, Mohd Hafizi Ahmad², Norhafezaidi Mat Saman², Osman Ayop³

¹Wireless Communication Centre, Faculty of Electrical Engineering, Universiti Teknologi Malaysia, 81310 Johor Bahru, Johor, Malaysia.

²Institute of High Voltage & High Current, Faculty of Electrical Engineering, Universiti Teknologi Malaysia, 81310 Johor Bahru, Johor, Malaysia.

³Department of Communication Engineering, Faculty of Electrical Engineering, Universiti Teknologi Malaysia, 81310 Johor Bahru, Johor, Malaysia.

*Corresponding author: ahmadzulbirri@graduate.utm.my, faridzubir@utm.my

Abstract: This paper presents a design for a log-periodic antenna tailored for the purpose of detecting partial discharges (PD) in high-voltage electrical equipment. Partial discharge events can result in insulation damage, leading to costly repairs and an elevated risk of electrical failures. While the challenge of distinguishing between PD signals and noise remains, the utilization of a log-periodic antenna is recommended due to its numerous inherent advantages, such as high gain and directional capabilities. An electromagnetic log-periodic antenna proves to be an optimal choice for PD detection and monitoring, offering a broad frequency coverage, heightened sensitivity, precise PD localization, and early-stage detection capabilities. Remarkably, the log-periodic antenna is proficient at efficiently transmitting approximately 90 percent of the received power, rendering it a highly effective diagnostic tool for safeguarding the integrity of high-voltage equipment.

Keywords: Partial discharge, Log-Periodic Antenna

© 2025 Penerbit UTM Press. All rights reserved

Article History: received 29 January 2024; accepted 2 July 2025; published 31 August 2025

1. INTRODUCTION

"Partial discharge" refers to an electrical discharge or spark that occurs between two conductive electrodes that are not in direct contact. In high-voltage equipment, the insulation system often faces degradation issues, primarily caused by partial discharge (PD) [1]. Therefore, monitoring PD is crucial, as it allows early detection of insulation weaknesses before they lead to catastrophic failures. PD events can contribute to energy losses and progressive insulation deterioration. As a result, reliable detection techniques are essential to determine the presence or absence of PD sources within the insulation system [2].

PD typically occurs when a small spark travels through a weak point in the insulation between conductive parts. It may arise at various locations within the insulation and usually indicates defects in the insulating material or the surrounding high-voltage equipment. While insulation aging is a contributing factor, PD can also originate in crevices, voids, or bubbles within dielectric liquids [1]. The presence of a gas-filled gap between conductors is a common condition for PD to occur.

To date, there are six techniques that are used for the detection, identification, and diagnosis of PD. These methodologies encompass electrical detection [3], electromagnetic detection [3], optical detection [4], acoustic detection [5], gas presence detection [6], and integrated detection [7]. The effectiveness of these techniques varies significantly. Despite the advantages of

electromagnetic detection, such as precise localization and immunity to low-frequency signals, it can be susceptible to electromagnetic interference. Electrical detection systems, while offering quantifiable results and ease of use, are prone to false alarms. Gas presence detection provides insights into the chemical composition related to PD but may pose challenges in calibration and necessitate offline testing. Acoustic emission detection, while effective in some cases, faces difficulties in accurately pinpointing PD sources due to interference from electromagnetic signals. Optical detection allows covert monitoring but presents challenges in PD calibration and detecting discharges in transparent materials. It is important to note that this study exclusively focuses on electromagnetic detection, specifically employing the Ultra-High Frequency (UHF) technique. This emphasis aligns with the primary theme of this research, centered on the utilization of log-periodic antennas for PD detection.

UHF signals can be detected using conical, spiral, and Vivaldi antennas [3, 8]. UHF sensors are the subject of extensive research since they have benefits that include immunity to low-frequency signals, an insignificant impact of signals caused by internal transformer construction, and the absence of corona-free pulse interference [9, 10]. Radio interference and switching events might make UHF detection more difficult.

For its measurements, the UHF electromagnetic technique depends on the PD activation of electrical

resonance at frequencies up to 1.5 GHz. This technique can also detect and pinpoint a PD source [11, 12]. The UHF method offers multiple benefits, for instance low decibel levels as a sequence of the transformer's shielding effect and extremely low signal losses [13]. The measurement frequency band of 100 MHz of such UHF process fits precisely between the 300 and 1500 MHz of the entire wavelength range, permitting it to avoid local interference over the entire range. Because the UHF sensor is linked within the transformer, this technology is noise-free. Secondary winding is safe and dependable against induced current since there is no electrical interrelation between the power transformer and the UHF sensor. The secondary winding of a power transformer is safe and reliable against induced current. Thus, the electromagnetic (EM) technique has proven effective in localizing multiple PD sources and identifying their unique characteristics through the use of feature extraction and denoising strategies. These strategies are used in PD detection through the EM signal approach to identify and analyze PD signals in power transformers accurately.

This paper proposes Log-periodic Antenna (LPDA) as the preferred detection method, stems from the necessity to address the diverse frequency range within PD signals [14]. External frequencies like GSM (900MHz) and TV (550MHz) pose interference challenges during PD detection. The LPDA emerges as an ideal solution due to its exceptional sensitivity to PD signals, capacity to encompass a wide spectrum, as well as its inherent directivity and high-power directional capabilities. These attributes collectively enable effective discrimination and isolation of PD signals amidst the presence of interfering frequencies, ensuring more precise and reliable detection [15].

2. DESIGN OF LOG-PERIODIC ANTENNA

The development of specifications for a log-periodic antenna designed for partial discharge (PD) detection requires careful consideration of several key parameters, as outlined in Table 1. One of the most important factors is defining the target frequency range, which spans from 400 MHz to 1.5 GHz to ensure adequate coverage of PD signals. A wide bandwidth is essential for capturing the full spectrum of PD emissions, while proper impedance matching is necessary to maximize signal reception and transmission efficiency. Antenna gain, which affects sensitivity, and directivity, which aids in accurately locating PD sources, are also critical design aspects. Impedance compatibility with the receiver system must be maintained for optimal performance, and the selection of polarization in which is linear or circular, should be based on the specific application environment. From a practical standpoint, compact and lightweight designs are preferred, especially for ease of installation and portability. Additionally, the radiation pattern must suit the intended monitoring area, and the choice of materials should ensure good electrical conductivity and long-term durability. The overall design process involves simulation, analysis, and optimization using professional tools such as CST Studio Suite to ensure the antenna meets all performance requirements for effective PD detection.

Table 1. Design specification of Log-Periodic Antenna

Type / Specification	Target
Operating Frequency	400 – 1500 MHz
Bandwidth	> 90%
Gain	> 4dB
Polarization	Linear
Radiation pattern	Directional

2.1 First design of Log-Periodic Antenna

The log periodic dipole antenna (LPDA) is constructed with a series of dipole elements that progressively decrease in size towards the rear. This characteristic is known as backfire radiation. At the back of the array, where the elements are largest, the element's length corresponds to half a wavelength at the lowest operating frequency. Equation 1, which is dependent on the scaling factor (τ), can be used to calculate the dimensions of the antenna, including its length (l), width (w), and distance (d) [16].

$$\tau = \frac{l_n}{l_{n+1}} = \frac{w_n}{w_{n+1}} = \frac{d_n}{d_{n+1}} \quad (1)$$

Subsequently, Equation 2 is employed to calculate the length of each element. In this equation, the actual propagation speed on the dipole, denoted as v , is obtained by utilizing Equation 3 [16].

$$l = 0.5 \times \frac{v}{f} \quad (2)$$

$$v = \frac{c}{\sqrt{\epsilon_r}} \quad (3)$$

The formula from (1) is used as a ratio for the length, width, and distance between elements. In order to use the ratio, the length needs to be calculated first by using formulas (2) and (3). By using the dielectric constant, which is 4.6, and the speed of light, 3×10^8 , the value for actual propagation speed, v , can be obtained. Thus, the length of the dipole antenna can be measured when divided by the chosen frequency.

To start with, the design specifications for the log periodic antenna, including the target frequency range, gain, directivity, impedance, and radiation pattern, are clearly defined. With these specifications in mind, the initial dipole antenna, often referred to as the "primary" or "driven" element, is designed based on Figure 1. This dipole is designed to resonate at the lowest frequency of the desired range, and its length is determined based on the target frequency. By choosing 400 MHz as the reference frequency, the length of the dipole can be calculated by using formulas (2) and (3).

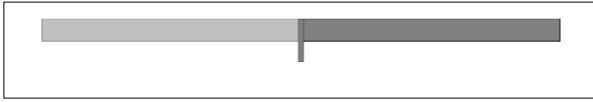


Figure 1. First element of antenna (400MHz)

Once the primary dipole is designed, the subsequent dipole antennas are created using frequency scaling. Each additional dipole is designed to resonate at progressively higher frequencies, and their lengths are determined by scaling factors (τ) applied to the primary dipole length. The spacing between adjacent dipoles gradually decreased as the frequency increases to maintain the desired impedance characteristics and radiation pattern. The element sizes may also vary along the antenna structure to achieve the desired frequency response. By increasing the targeted frequency range of the log periodic antenna by 150 MHz, it was determined that the antenna would require a total of eight dipole elements. This theoretical calculation takes into account the desired frequency coverage of 400MHz to 1500MHz.

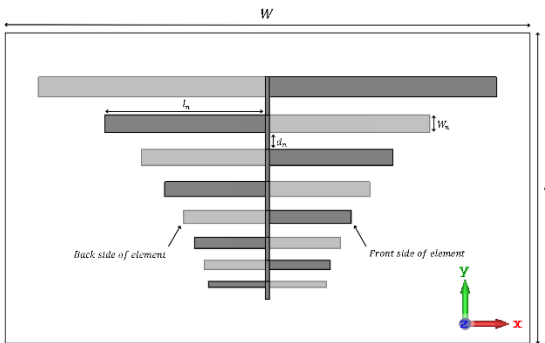


Figure 2. Front and back view of the initial antenna

Table 2. Parameters of initial antenna

Elements No. (n)/ Frequency (MHz)	Length of element, l_n (mm)	Width of element, w_n (mm)	Distance between element, d_n (mm)
1 / 400	159.84	14.00	12.50
2 / 550	112.60	12.50	12.00
3 / 700	86.91	11.00	11.50
4 / 850	70.28	10.50	10.00
5 / 1000	57.94	9.00	9.50
6 / 1150	49.82	7.50	9.00
7 / 1300	42.80	6.00	8.50
8 / 1450	39.50	4.50	8.00

The dipole antennas were compiled based on parameters in Table 2 to form the log periodic antenna as shown in Figure 2, a simulation was conducted to evaluate its performance. However, the results obtained did not align with the expected outcomes, indicating the need for

optimization to meet the desired specifications.

2.2 Final design of Log-Periodic Antenna

The optimization process involved analyzing the simulation data, identifying areas of deviation or underperformance, and making adjustments to improve the antenna's characteristics. Various parameters were considered for optimization, including the dipole lengths, element spacing, and feed network design.

Various optimization techniques were employed to enhance the antenna's performance. This involved modifying the dipole lengths to better match the desired frequencies, adjusting the element spacing to achieve the desired radiation pattern and impedance, and optimizing the feed network for improved signal distribution.

Once the modifications were implemented (as in Table 3), the log-periodic antenna as shown in Figure 3 is re-simulated to assess the impact of the changes. This iterative process of optimization and simulation continued until the antenna's performance met the desired specifications. Several rounds of adjustments, simulations, and evaluations were conducted to fine-tune the antenna design. In order to improve the antenna's ability to resonate at different frequencies within the desired range, four additional elements were added. This adjustment allowed for better coverage of the frequency spectrum and improved the antenna's overall performance.

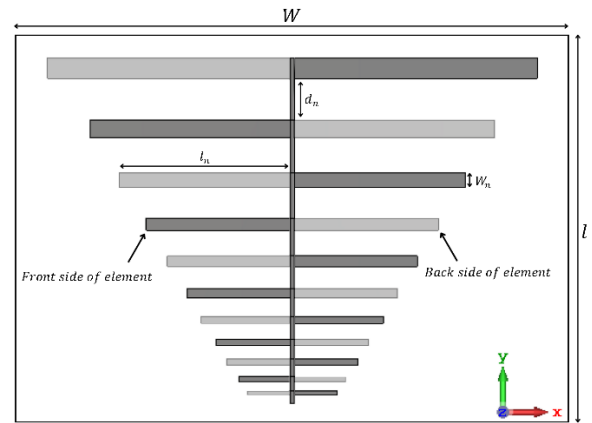


Figure 3. Front and back view of the antenna after optimization

Table 3. Parameters of optimized antenna

Number of elements, n	Length of element, l_n (mm)	Width of element, w_n (mm)	Distance between element, d_n (mm)
1	161.00	13.50	27.80
2	133.50	11.50	23.50
3	113.40	9.76	20.24
4	96.20	8.24	17.16
5	81.20	7.04	14.56

6	68.80	6.00	12.30
7	58.50	5.04	10.56
8	49.50	4.32	8.88
9	41.80	3.68	7.62
10	34.53	3.40	6.21
11	28.00	3.19	5.00

After running simulations and making the necessary optimizations, the next step was to build a prototype of the antenna, as shown in Fig. 4. The antenna was fabricated on the FR4 substrate printed circuit board (PCB) with a thickness of 1.6 mm, a dielectric constant of 4.4, and a dielectric loss ($\tan \delta$) of 0.02. The radiating patch and ground plane were made from copper with a thickness of 0.035 mm.



Figure 4. Front and back view of the fabricated antenna after optimization

3. SIMULATION RESULTS AND DISCUSSION

The antenna prototype is subjected to testing and analysis, including the measurement of S-parameters and VSWR.

The initial simulation showed that in some parts of the 400 MHz to 1500 MHz range, the return loss was higher than -10 dB, indicating poor signal reception at those frequencies. Since effective PD detection requires a return loss better than -10 dB across the entire band, further optimization was needed. This led to efforts to refine the antenna design to improve performance in the affected frequency range.

After applying optimization techniques to the antenna design, the return loss improved significantly, reaching about -37 dB. This means the antenna now works well within the important frequency range of 400 MHz to 1500 MHz, with return loss staying below -10 dB as required. These improvements show that the antenna performs better and is a strong and reliable option for partial discharge (PD) detection in this frequency range.

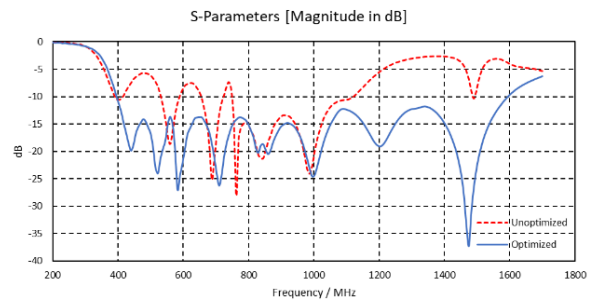


Figure 5. Comparison of simulation between initial and after optimization

Figure 5 shows the comparison between the initial design and with optimized version after some adjustments. The initial design didn't meet the standards needed to detect partial discharge properly. So, it got refined until it met all the requirements. The final version of the antenna, the improved one, was then used to measure partial discharge accurately.

The S-parameters and VSWR were measured using a Rohde & Schwarz ZVL network analyzer. The measured return loss and VSWR were then compared with the simulated results, as shown in Figures 6 and 7. The comparison shows that the measured and simulated S11 values match closely, indicating good and reliable results.

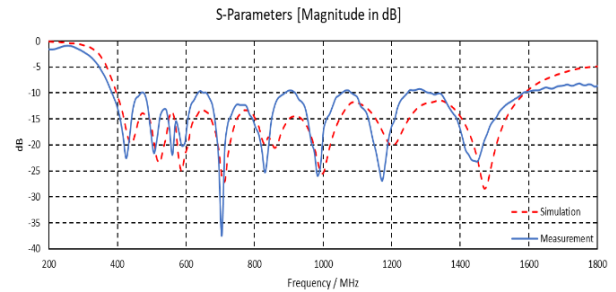


Figure 6. Comparison of simulation and measurement results

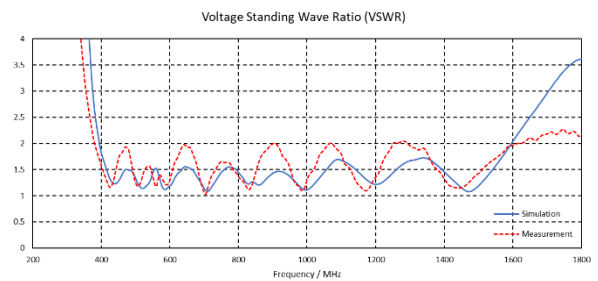
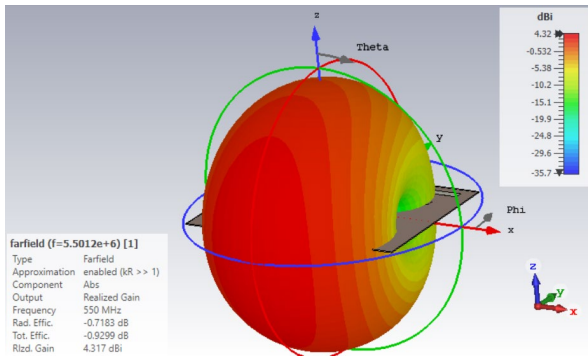
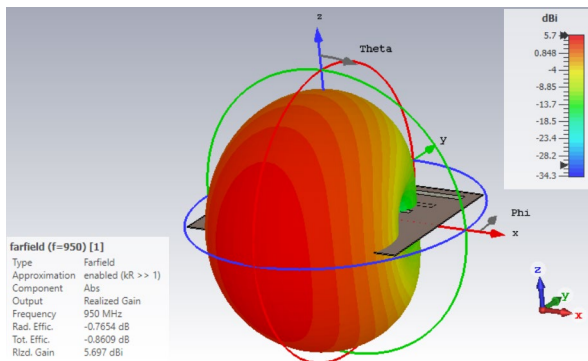


Figure 7. VSWR result between simulation and measurement

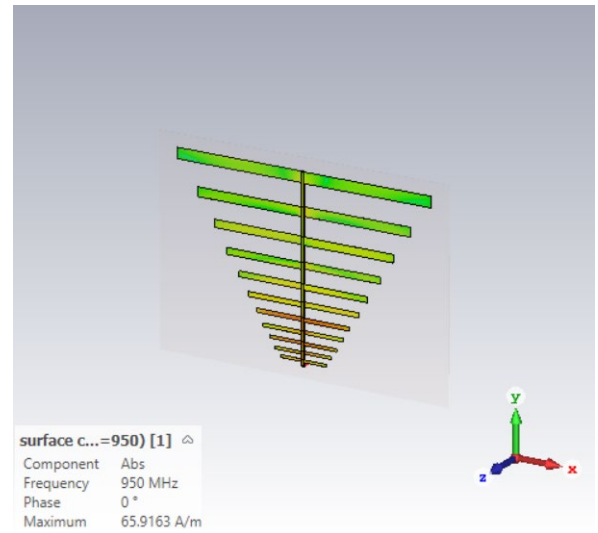


(a)



(b)

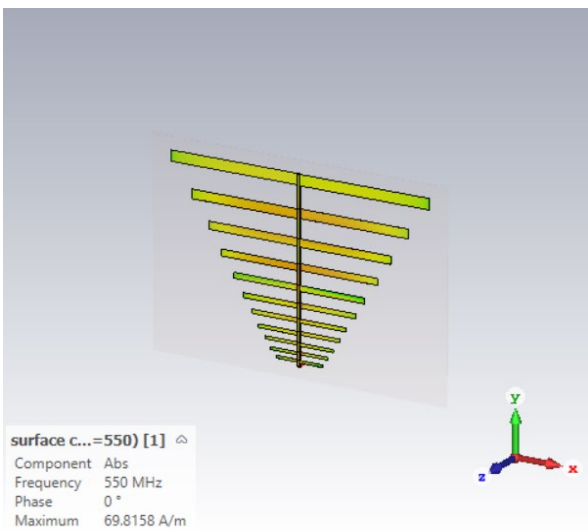
Figure 8. 3D radiation pattern for (a) 550MHz and (b) 950MHz



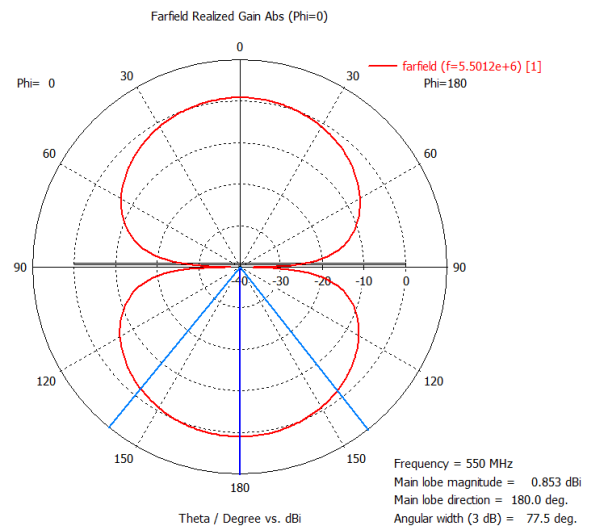
(b)

Figure 9. Current distribution for (a) 550MHz and (b) 950MHz

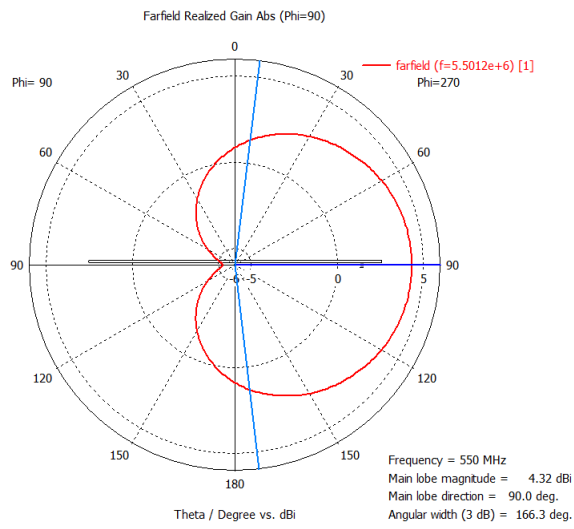
Figure 9 presents the current distribution along the log-periodic antenna. The simulation results confirm that the antenna operates effectively, particularly at lower frequencies where the larger antenna elements are active, in line with the design concept. The current distribution is shown at two frequencies which are at 500 MHz and 950 MHz, demonstrating the antenna's ability to perform across a wide frequency range, which reflects its broad bandwidth capability.



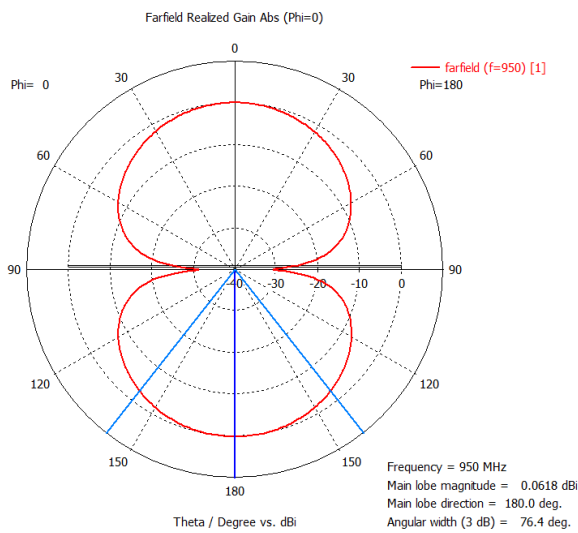
(a)



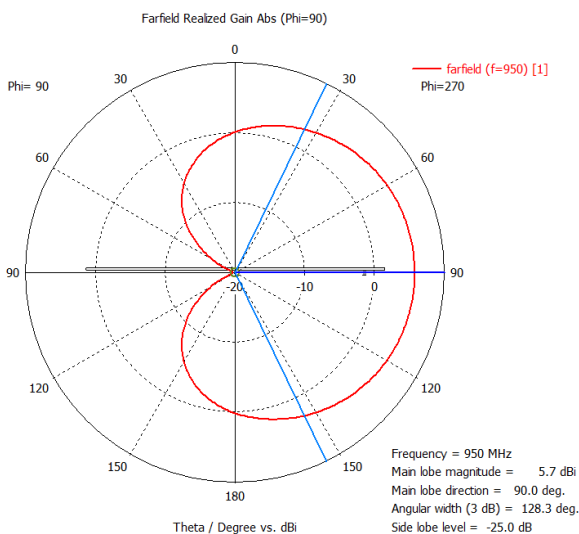
(a)



(b)



(c)



(d)

Figure 10. Simulated radiation pattern at: 550MHz (a) E-plane (b) H-plane, 950MHz (c) E-plane (d) H-plane

The simulated radiation pattern of the proposed antenna is depicted in Figure 10 for the xz-plane (as shown in Figure

10(a) and (c)) and in the yz-plane (as depicted in Figure 10(b) and (d)). These patterns exhibit directional characteristics, each in their respective planes.

Table 4. Realized gain of the Log-Periodic Antenna

Frequency, MHz	Realized Gain, dBi
550	4.317
950	5.697

In this section, Table 4 presents the realized gain of the log periodic antenna at 550 MHz and 950 MHz. It's observed that the gain rises with an increase in frequency. Additionally, the angular width, as depicted in Figure 10 (H-plane), decreases from 166.3° at 550 MHz to 128.3° at 950 MHz due to the frequency escalation. Consequently, an increase in frequency results in a more directional antenna with higher gain.

4. CONCLUSION

In summary, the developed log periodic antenna has demonstrated significant promise within the frequency range associated with partial discharge signals (400MHz – 1500MHz). Its capacity to cover a broad frequency spectrum coupled with heightened sensitivity renders it well-suited for precise localization and early-stage detection of PD in high-voltage power equipment. This stands in contrast to the conventional method employing a monopole-type antenna, which typically exhibits lower gain. The proposed antenna design effectively mitigates the risk of detecting extraneous signals from GSM/TV, thereby enhancing the accuracy and reliability of PD signal detection and localization in the specified frequency range.

ACKNOWLEDGMENT

This work was supported by the Higher Institution Centre of Excellence, Ministry of Higher Education Malaysia through the Wireless Communication Centre, Universiti Teknologi Malaysia (UTM) under Grant R.J130000.7823.4J610; in part by the UTM Fundamental Research under Grant Q.J130000.3823.23H92; and in part by the Faculty of Engineering, Multimedia University, Cyberjaya, Selangor, Malaysia.

REFERENCES

- [1] Feger, R., et al. *Nonconventional UHF sensors for PD measurements on GIS of different designs*. in *PowerCon 2000. 2000 International Conference on Power System Technology. Proceedings (Cat. No. 00EX409)*. 2000. IEEE.
- [2] Gorgan, B., et al. *Monitoring and Diagnosis of Electrical Equipment Insulation with the Support of Combined Conventional and Alternative Partial Discharge Methods*. in *2022 9th International Conference on Condition Monitoring and Diagnosis (CMD)*. 2022. IEEE.
- [3] Darwish, A., et al., *On the electromagnetic wave behavior due to partial discharge in gas insulated*

- switchgears: State-of-art review*. IEEE Access, 2019. 7: p. 75822-75836.
- [4] Biswas, S., et al., *A methodology for identification and localization of partial discharge sources using optical sensors*. IEEE Transactions on Dielectrics and Electrical Insulation, 2012. **19**(1): p. 18-28.
 - [5] Refaat, S.S., et al. *A review of partial discharge detection techniques in power transformers*. in *2018 Twentieth International Middle East Power Systems Conference (MEPCON)*. 2018. IEEE.
 - [6] Dai, J., et al., *Dissolved gas analysis of insulating oil for power transformer fault diagnosis with deep belief network*. IEEE Transactions on Dielectrics and Electrical Insulation, 2017. **24**(5): p. 2828-2835.
 - [7] Wang, X., et al., *Acousto-optical PD detection for transformers*. IEEE transactions on power delivery, 2006. **21**(3): p. 1068-1073.
 - [8] Wiesbeck, W., et al. *Influence of antenna performance and propagation channel on pulsed UWB signals*. in *2007 International Conference on Electromagnetics in Advanced Applications*. 2007. IEEE.
 - [9] Jiang, T., et al., *Improved bagging algorithm for pattern recognition in UHF signals of partial discharges*. Energies, 2011. **4**(7): p. 1087-1101.
 - [10] Sinaga, H.H., B. Phung, and T. Blackburn, *Partial discharge localization in transformers using UHF detection method*. IEEE Transactions on Dielectrics and Electrical Insulation, 2012. **19**(6): p. 1891-1900.
 - [11] Judd, M.D., L. Yang, and I.B. Hunter, *Partial Discharge Monitoring for Power Transformers Using UHF Sensors Part 2: Field Experience-The results of PD tests on power transformers provide sufficient evidence to justify making provision*. IEEE Electrical Insulation Magazine, 2005. **21**(3): p. 5-13.
 - [12] Judd, M.D., L. Yang, and I.B. Hunter, *Partial discharge monitoring of power transformers using UHF sensors. Part I: sensors and signal interpretation*. IEEE Electrical Insulation Magazine, 2005. **21**(2): p. 5-14.
 - [13] Chai, H., B.T. Phung, and S. Mitchell, *Application of UHF sensors in power system equipment for partial discharge detection: A review*. Sensors, 2019. **19**(5): p. 1029.
 - [14] Muru, A. and E. Setijadi. *Design a Microstrip Log-Periodic Dipole Antenna for Partial Discharge Detection in the VHF and UHF Frequency Bands*. in *2023 International Seminar on Intelligent Technology and Its Applications (ISITIA)*. 2023. IEEE.
 - [15] Cui, Z., et al., *Wideband UHF antenna for partial discharge detection*. Applied Sciences, 2020. **10**(5): p. 1698.
 - [16] Balanis, C.A., *Antenna theory: analysis and design*. 2016: John wiley & sons.